Journal of Applied Electrochemistry **32**: 1391–1396, 2002.

Nucleation during electrocrystallization of cobalt on glassy carbon (GC)

K.G. MISHRA[1,*] P. SINGH[2] and D. MUIR[3]
[1]*Regional Research Laboratory (C.S.I.R), Bhubaneswar 751 013, India;*
[2]*Division of Sciences and Engineering, Murdoch University, WA 6150, Australia;*
[3]*Division of Minerals, C.S.I.R.O, WA 6102, Australia;*
*(*author for correspondence, e-mail: drkgmishra@yahoo.com)*

Received 8 May 2001; accepted in revised form 10 April 2002

Key words: chronoamperometry, cobalt, electrocrystallization, glassy carbon, nucleation

Abstract

A glassy carbon (GC) static disc electrode substrate was employed for both chronoamperometry and to study the morphological growth behaviour of cobalt in sulfate solutions containing 0.10 M and 0.50 M Co^{2+}, at pH 2.5, and 60 °C. The effect of potentiostatic pulses on the initial stage of electrodeposition of cobalt is reported. The early stages of metal deposition were found to be controlled by three-dimensional instantaneous nucleation followed by hemispherical growth. The experimental findings for the growth mechanism matched well with the theoretical results and the 3D-growth of cobalt nuclei was confirmed by scanning electron microscopy (SEM).

1. Introduction

Extensive work on the electrocrystallization of cobalt has been carried out by many authors [1–14] on different electrode materials from aqueous solutions. However, the first stage of the nucleation of crystallites on the substrate surface is, in fact, an important aspect of any metal deposition process [15–19]. Such early stages of electrochemical phase transformation are usually associated with a 1, 2 or 3 dimensional nucleation process [4–6, 14, 19]. The formation and growth of an electrodeposits phase is a complex nucleation process and several principles have been proposed [2, 4, 10, 14] to describe the cathodic deposition of metal especially when the substrate and the metals are the same [3, 6, 11, 15, 17]. In other cases it has been shown that electrodeposition reactions are associated with a nucleation process. In this respect the classical vapour phase nucleation theory [8, 9] system involving electrochemical deposition is relatively simple requiring the dimensionless supersaturation parameters, S, in terms of the overpotential, η. That is,

$$S = \frac{zF}{RT\eta} \tag{1}$$

The nucleation rate is represented by a rate constant, which may be expressed by the following relationship,

$$\mathrm{J} = A\exp\left(\frac{-B}{\eta^2}\right) \tag{2}$$

where B contains several constant terms [9]. According to this equation a critical overpotential (corresponding to a critical supersaturation for the homogeneous phase theory) is observed before the onset of nucleation. Both the metal ion and the substrate material control this critical overpotential. During the nucleation study it is observed that the nuclei are randomly distributed crystallites of near identical size, growing under mass-transfer control [4, 6, 10]. Rising transients are observed which reflect the increase in current as each nucleus grows in size and with it the total area of electroactive surface. Well before the overlap of the diffusion zones of adjacent nuclei, the total current can be identified with the sum of the individual nucleus currents [6].

$$I_{N,t} = \sum I_{i,t} \tag{3}$$

where $I_{i,t}$ is the current to an individual nucleus i, and N is the total number of nuclei.

Furthermore, when the nucleation process takes place 1, 2 or 3-dimensional morphologies can be observed for the growth of nuclei on suitable nucleation sites. Whatever the growth morphology, two different regimes can be established. For the first one, the rate-determining step is represented by the metal incorporation into the growth point whilst for the second one the rate-determining step is the mass transfer of the depositing metal ions towards the surface of the growth nucleus.

The kinetics of electrochemical formation of cobalt has been examined [17, 21]. In all cases it has been seen that nucleation of the new phase occurs at preferred sites

and that the centres formed subsequently grow into two or three dimensions.

The present paper gives the results of an investigation of the early stages of electrodeposition (the nucleation) of cobalt using a current–time transient technique at constant potential on a glassy carbon (GC) electrode substrate in aqueous sulphate solution.

2. Experimental details

A conventional three electrode cell system was used for all the experiments. The working electrode was prepared by mounting a vitreous carbon rod of 0.0556 cm^2 cross sectional area (2.66 mm dia.) in a Teflon holder. The vitreous carbon working electrode was chosen as it is a good neutral substrate with no influence on the structure or the orientation of three-dimensional cobalt nuclei. The exposed electrode surface was polished to a mirror finish using alumina powder successively up to fine (1 μm) size as the reproducibility of the results obtained depends greatly on the quality of polishing. Any impurities adsorbed on the surface may be an active subcentre for recrystallization and change the shape of the transient recorded.

The electrolyte for cyclic voltammetry and chronoamperometry study was prepared from analytical grade cobalt(II) sulfate hepta hydrate $CoSO_4 \cdot 7H_2O$, using ultrapure water (Millipore Milliq system). The pH of the solutions was adjusted using analytical grade sulfuric acid. The temperature of the solutions, unless otherwise mentioned, were at 60 °C.

The working mirror finish surface was dipped into the solution maintained at pH 2.5 and 60 °C and just previously deoxygenated by sparging with high purity nitrogen for 10 min. The counter electrode was a spiral platinum wire and all the potentials were recorded with respect to an Ag/AgCl electrode connected to a Luggin capillary containing sulfate deposition solution. This avoided contamination of solution with chloride ions which may easily adsorb on the initial deposit, modifying the cobalt growth mechanism. The equipment for this study consisted of an EG and G Princeton 175 universal programmer and model 173 potentiostat coupled with an X–Y recorder to generate current–time transient curves. The morphology of the nucleation of cobalt was investigated using a Philips XL30 scanning electron microscope.

3. Results and discussion

3.1. *Current–time characteristics*

The current–time transients were recorded by applying a potential pulse from an initial potential value for which zero or minimum current was detected. The shapes of the current–time profiles obtained in solution containing 0.10 M and 0.50 M Co^{2+} were related to nucleation and three-dimensional growth behaviour. The interesting feature of the current–time transient is the rising region of the peak, which corresponds to the density of nuclei before overlapping of the first monolayer of the growing nuclei occurs. This region therefore can be used to derive the kinetics of the nuclei growth. The time t_{max}, at current maxima (I_{max}) in the current–time transient curves, can then be related to the time at which full coalescence of the crystallite occurs.

The overvoltage/potentiostatic pulses applied for this purpose were selected from the cyclic voltammograms of cobalt deposition on glassy carbon electrode at different [Co^{2+}] as shown in the Figure 1(a) and (b). The linear region (A) is followed by a point (B) where the current increases sharply corresponding to the nucleation potential. Afterwards at potential reversal, in region (C) the current falls and crosses the region (A). The region (B–C) corresponds to the nucleation region and the point (D) on the potential axis, where the reverse sweep crosses the region (A), is the nernstian potential. The region (D–B) represents the nucleation overpotential. Hence, the potentiostatic pulses of present interest for current–time transients are between the nucleation potential and the reversal potential.

The typical current–time behaviour is presented in Figure 2 [22]. There are three characteristic regions in the current–time curves. The first is an initial pulse of very short duration corresponding to a high current intensity which is probably related to the double layer charging transient. This is then followed by a second region where a short and essentially small constant

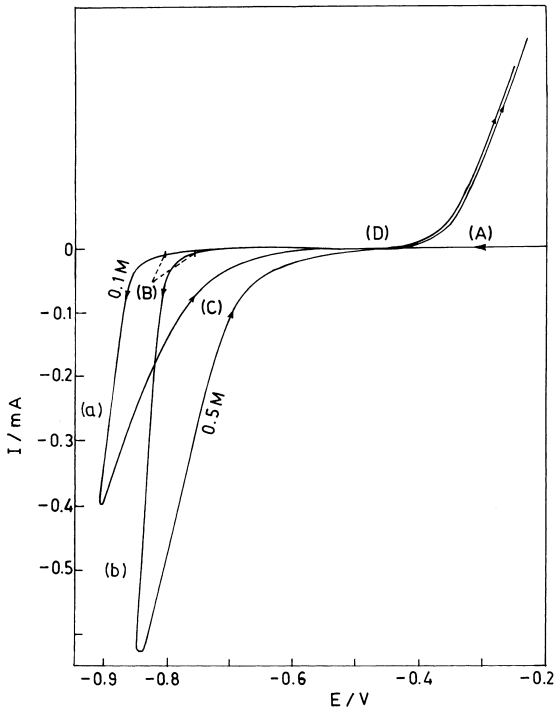

Fig. 1. Cyclic voltammogram of cobalt deposition in a sulphate solution containing (a) 0.1 M and (b) 0.5 M Co^{2+} on glassy carbon (GC) electrode substrate at pH 2.5, and 60 °C.

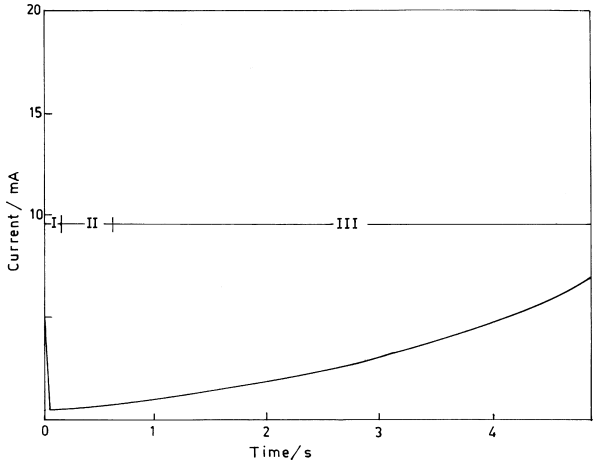

Fig. 2. A typical current–time transient in 40 g l^{-1} Cu^{2+}, 180 g l^{-1} H_2SO_4 onto a stainless steel RDE at an applied potential of −0.50 V, $t = 40$ °C, area of the ss electrode 0.512 cm^2 and rotation speed 500 rpm [22]. Regions: (I) capacitative current; (II) induction; (III) nucleation and growth.

current is observed indicating an induction period. As cobalt nucleates and grows, the current increases with time to give the third region. The value of the critical overpotential is strongly dependent on the particular metal and substrate involved and usually ranges between 10 mV and 100 mV [5, 7, 14, 19].

3.2. *I/t characteristics of cobalt*

The sets of I/t transients measured at different cobalt concentrations and potentiostatic pulses for electrodeposition of cobalt obtained on the GC electrode substrate are presented in Figure 3. The results obtained by applying different potentiostatic pulses for a period of 120 s in a solution containing 0.10 and 0.50 M Co^{2+} are presented in Figure 3(a) and (b), respectively. The respective potentiostatic pulse for that particular curve is given on the curve itself. In all the transient curves, a maximum current I_{max} is observed at time t_{max} that is dependent both on the pulse potential and on the solution cation concentration. The current then falls and maintains a near constant value up to 120 s. The results show that the potentiostatic pulse and the concentration of the metal ion depositing play an important role during electrocrystallization, as found by comparing Figure 3(a) and (b). The current maxima (I_{max}) values in the current–time transient curves of 0.50 M Co^{2+} solution are greater than in solution of 0.10 M Co^{2+} using the same potentiostatic pulses. This t_{max} value can be related to the time at which full coalescence of the crystallite occurs.

From the results of t_{max} and I_{max} (Table 1), it is found that, with an increase in Co^{2+}, concentration and a more negative potentiostatic pulse, the I_{max} value increases reflecting a greater rate of nucleation of cobalt on the GC electrode substrate. At −0.85 V in 0.50 M Co^{2+}, t_{max} is significantly higher in comparison to others since it takes 10 s to reach the I_{max} value of 0.95 mA. This may be due to the fact that the potentiostatic pulse is close to the nucleation potential ($\eta = 60$ mV). In all other potentiostatic pulses the t_{max} value lies between 4–6 s. At any particular potentiostatic pulse in 0.10 M Co^{2+}, the I_{max} value is lower than the I_{max} value at

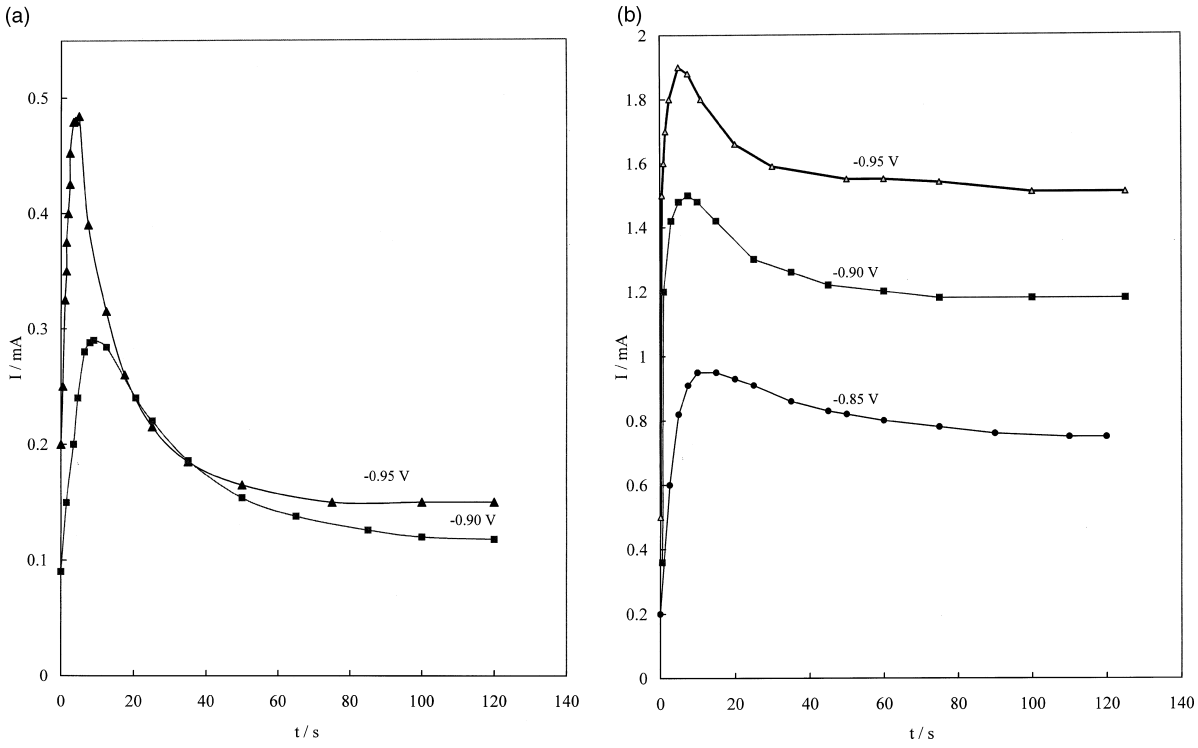

Fig. 3. Current–time transient curves for 120 s of deposition on GC electrode substrate in solutions at pH 2.5 and 60 °C containing (a) 0.1 M Co^{2+} + 0.08 M Na_2SO_4, (b) 0.50 M Co^{2+} + 0.08 M Na_2SO_4.

Table 1. Effect of Co^{2+} concentration and potentiostatic pulse voltages on I_{max} and t_{max}

Concentration /M	Potentiostatic pulse /V	t_{max} /s	I_{max} /mA
0.10	−0.90	6.3	0.382
	−0.95	4.0	0.46
0.50	−0.85	10.0	0.95
	−0.90	6.5	1.5
	−0.95	5.0	1.9

0.50 M Co^{2+}. This indicates that at increased concentration, the greater I_{max} value may be attributed to the fact that there are more nucleation sites of cobalt on the GC electrode substrate (Equation 3).

3.3. *Mechanism of cobalt growth*

The rising part of the current–time transient curve is needed to determine the kinetics and mechanism of nuclei growth, and corresponds to the intensity before overlapping of the growing nuclei. Hence, the particular shape of the current–time transients strongly suggests that a nucleation process is involved in the electrodeposition of cobalt. The first part of each current–time transient is largely a charging current that decays during nucleation. The rising portion reflects the increase in current because each independent nucleus grows in size and subsequently increases the total area of electroactive cobalt surface. In the latter stage of the transient the diffusion zone around the nuclei overlap and one diffusion layer is formed, the shape of which will depend on the electrode geometry. Consequently the current falls, and approaches that corresponding to the diffusion controlled process.

Two types of nucleation may occur in the case of a mass transfer controlled process [14, 22]: (i) instantaneous and (ii) progressive. The equations are, respectively,

$$I_{inst} = zF\pi(2DC)^{3/2}M^{1/2}N_0t^{1/2}\rho^{-1/2} \quad (4)$$

$$I_{prog.} = 2/3zF\pi AM^{1/2}(2DC)^{3/2}t^{3/2}\rho^{-1/2} \quad (5)$$

Table 2. Probable values of n for different mechanism

Nucleation type	Progressive				Instantaneous	
Mechanism	Kinetics		Diffusion		Kinetics	Diffusion
Morphology	2D	3D	3D	2D	3D	3D
n values	2	3	1.5	1	2	0.5

where A is defined as $A'N_0$ (A' is the steady state nucleation rate constant per site also known as nucleation rate constant and N_0 is the number of nuclei) is the adjusted nucleation rate constant, M, ρ, D, C and t are the atomic weight, density of the depositing metal, the diffusion coefficient, the concentration of the electrodepositing species and the time of nucleation, respectively, and all other terms have their usual meaning.

The probable values of n for different mechanisms are summarized in Table 2 for the analysis of results where n represents the slope of the log I against log t. Thus, the mechanism of the deposition process can be predicted from the slope of the log I/log t curve as shown in Table 2. Furthermore, the growth of the nuclei can be predicted as correlated from the morphological pattern obtained through SEM.

The actual values of the measured slopes for cobalt are presented in Table 3. Since the values differ slightly, it is assumed that the slope depends primarily on the geometry and type of nucleation. The results obtained from experimental findings match well with the theoretical value of 0.5, which suggests (according to Equations 4 and 5) that the particular process involved is one of instantaneous three-dimensional nucleation with hemispherical growth and is diffusion controlled. Direct evidence for the morphological pattern of the nucleation of cobalt for this model was obtained by scanning electron microscopy examination of the electrode surface.

3.4. *Morphology of cobalt deposit*

The three-dimensional nucleation obtained by SEM is shown in Figure 4(a)–(f). The nucleation at different times, but at a particular potentiostatic pulse potential as shown in the Figure, indicates the three-dimensional growth pattern of cobalt on the GC electrode substrate. At 0.5 M Co^{2+} the measured log I/log t slopes are close

Table 3. Slopes obtained from log I/log t curves at different potentiostatic pulses and [Co^{2+}]

[Co^{2+}] /M	Potentiostatic pulse /V	Slope from equation	Measured slope	Visual observation		
				3 s	30 s	120 s
0.10	−0.90	0.5	0.6	Not possible*	Nice†	Good‡
	−0.95	0.5	0.47	Not possible*	Nice†	Good‡
0.50	−0.85	0.5	0.55	Not possible*	Nice†	Good‡
	−0.90	0.5	0.41	Very thin deposition	Nice†	Good‡
	−0.95	0.5	0.34	Very thin deposition	Nice†	Good‡

* Detection: 'impossible'.
† Surface coverage: 'nice'.
‡ Amount of deposition: 'good'.

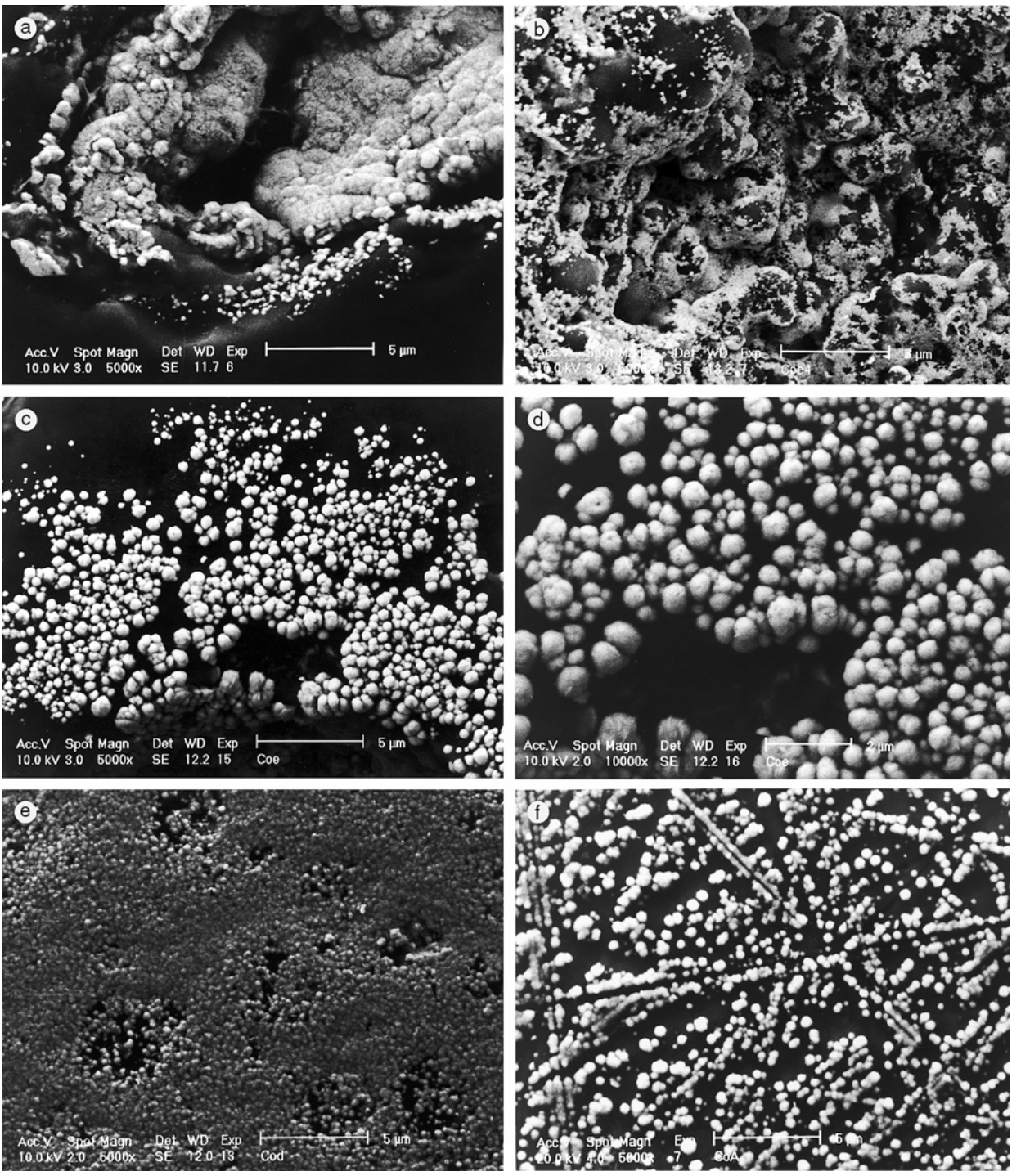

Fig. 4. Scanning electron micrographs of nucleation of cobalt at different potentiostatic pulse voltages and period of deposition on GC electrode substrate in sulphate solutions containing 0.1 M Co^{2+} + 0.08 M Na_2SO_4 at pH 2.5, and 60 °C. (a) 5 s at −0.90 V, (b) 20 s at −0.90 V, (c) 30 s at −0.90 V, (d) 30 s at −0.90 V, (e) 120 s at −0.90 V and (f) 30 s at −0.95 V.

to the theoretical value of 0.5 for each potentiostatic pulse of −0.85, −0.90, and −0.95 V. This indicates that there is an instantaneous nucleation process that is under diffusion control, but the nucleation has a three dimensional morphological pattern. Deposition of cobalt for 5 and 20 s (Figure 4(a) and (b)) shows the same discrete and distributed spherical deposit. After 30 s deposition on the GC electrode from 0.1 M Co^{2+} (Figure 4(c)) the deposit again shows discrete and well distributed spherical cobalt, which is still well defined at ×10 000 magnification (Figure 4(d)). However, at 120 s duration, the nuclei overlap and the substrate surface develops a smooth appearance (Figure 4(e)). A similar phenomenon was observed at a potentiostatic pulse of −0.95 V where the deposition continues for only 30 s. A well-nucleated spherical cobalt deposit with three-dimensional growth is observed covering the entire substrate surface (Figure 4(f)).

Thus, the chronoamperometric study and experimental findings closely fit the mechanism of the diffusion-controlled instantaneous nucleation with 3D-growth. The n values from Equation 4 provide a close fit with the experimental findings, and the 3D-growth of cobalt nuclei is further confirmed from Scanning electron microscopy.

4. Conclusions

The following findings can be drawn from the above study.

(i) The operating potentials in both 0.1 and 0.5 M Co^{2+} are under diffusion control.

(ii) The slope of the log I/log t graph at different operating potentials in both 0.1 and 0.5 M Co^{2+}, is close to the theoretical value of 0.5 for a nucleation mechanism that is instantaneous diffusion controlled having a 3D-growth pattern.

(iii) Scanning electron microscopy further confirms that there is a 3D morphological growth of cobalt on the GC electrode substrate.

Acknowledgements

The authors extend their thanks to the Australian Government for providing financial support under the TIL program to carry out the research work at Murdoch University, Perth. One of the authors, Dr Mishra is grateful to the HRD, CSIR (New Delhi), Dr R.P. Das, Head, H&EM Division, and the then Director, RRL (Bhubaneswar) for their support by sanctioning leave to travel to Australia. Dr Mishra is indebted to Dr V.N. Mishra, Director, R.R.L., Bhubaneswar, Orissa, for permission to publish this work.

References

1. I.N. Stranski, *Z. Physik. Chem.* **136** (1928) 259.
2. I.N. Stranski and R. Kaishev, *Z. Physik.* **36** (1935) 393.
3. M. Volmer, *Z. Physik.* **22** (1921) 646.
4. D.J. Astely, J.A. Harrison and H.R. Thirsk, *Trans. Fraday. Soc.* **64** (1968) 172.
5. M. Fleischmann and H.R. Thirsk, *Electrochim. Acta* **2** (1960) 123.
6. G.A. Gunawardna, G.J. Hills and I. Montenegro, *Electrochim. Acta* **23** (1978) 693.
7. R.D. Armstrong, M. Fleischmann and H.R. Thirsk, *J. Electroanal. Chem.* **11** (1966) 208.
8. O. Volmer, *Z. Physik. Chem.* **119** (1926) 277.
9. T.E. Gurz and M. Volmer, *Z. Physik. Chem. Abt.* **A157** (1931) 165.
10. D.J. Hills, D.J. Schriffrin and J. Thor, *Electrochim. Acta* **19** (1974) 65.
11. R. Kaischev and Mutaftchiew, *Electrochim Acta* **10** (1965) 643.
12. S. Toschev and I. Markov, *Electrochim. Acta* **12** (1967) 281.
13. A. Milechev, E. Vassileva and V. Keratov, *J. Electroanal. Chem.* **107** (1980) 337.
14. M. Fleischmann and H.R. Thirsk, *in* P. Delahay (Ed.), 'Advanced Electrochemistry and Electrochemical Engineering', **Vol. 3** (Academic Press, New York, 1963), p. 123.
15. R. Beratazzoli and D. Pletcher, *Electrochim. Acta* **38** (1993) 671.
16. E. Gomez, M. Marin, F. Sanz and E. Valles, *J. Electroanal. Chem.* **422** (1997) 139.
17. M.S. Cruz, F. Alanzo and J.M. Palacois, *J. Appl. Electrochem.* **23** (1993) 364.
18. E. Souteyrard, G. Maruin and D. Merciner, *J. Electroanal. Chem.* **161** (1984) 17.
19. G. Guranawardna, G. Hills, I. Montenegro and B. Scharifker, *J. Electrochem. Soc.* **138** (1982) 225.
20. I. Bimaghra and J. Crouiser, *Mater. Chem. Phys.* **21** (1989) 109.
21. J. Yu, H. Cao, Y. Chen, I. Kang and H. Yang, *J. Electroanal. Chem.* **474** (1999) 69.
22. M. Sun and T.J. O'Keefe, *Metall. Trans. B* **23** (1992) 591.